

EXPERIMENTAL RESEARCH ON FLOW SEPARATION CONTROL USING SYNTHETIC JET ACTUATORS

E. Koopmans* & H.W.M. Hoeijmakers*
*University of Twente, Enschede, The Netherlands,

Keywords: *Aerodynamics (Flow Control, High Angle of Attack, Wind Tunnel Testing)*

Abstract

Airplane wings can suffer from flow separation, which greatly decreases their aerodynamic performance. The flow separates due to the boundary layer possessing insufficient momentum to engage the adverse pressure gradient along the airfoil surface. Flow separation control actively influences the flow such that flow separation is delayed and airfoil performance is improved.

In this research flow separation control is applied on a 2D wing with a NACA0018 section with a 0.165 m chord using tangentially directed synthetic jets. The actuators are located inside the wing and the jet exits from a slot in the upper wing surface. The synthetic jet inhales the low momentum air in the boundary layer during instroke and during the outstroke the air adds momentum to the boundary layer.

The actuator, with a piezo-electric diaphragm, has a slot width of 0.25 mm. With this design jet velocities up to 65 m/s have been achieved at an optimum actuation frequency of 900 Hz.

A spanwise row of ten actuators is placed inside the wing, such that the slots cover 66% of the wing's span. During wind tunnel experiments forces have been measured using a balance.

The tests have been performed at a fixed free stream velocity of 25 m/s ($Re_c = 2.73 \times 10^5$) and for various actuation frequencies and jet velocities.

It is shown that for given actuation frequency a higher jet velocity results in a higher maximum lift coefficient and a corresponding higher stall angle. However, for the performance of the synthetic jet actuation, actuation frequency proves to be of greater importance than jet velocity. The best actuation frequency in combination with the maximum jet velocity possible with the

present actuator is a dimensionless frequency F^+ of 5.9 (1300 Hz) and a momentum coefficient c_μ of 0.0014 (maximum jet velocity 32.9 m/s and Velocity Ratio of 1.32). Using these actuation parameters the lift coefficient is increased by 12% and the stall angle by 22%.

1 Introduction

For an airplane to takeoff and land, it is required to produce high levels of the lift coefficient at low speeds in order to be able to fly. Current airplanes achieve this by employing systems that are deployed only during takeoff and landing. These systems usually consist of a movable leading edge slat and trailing edge flaps, transforming the wing in a multi-element system, effectively increasing camber and chord length and resulting in high lift coefficients.

Fig. 1 shows an example of the section of such a wing.



Fig. 1. Section of a high-lift wing section with a leading-edge slat and single-slotted trailing-edge flap (adapted from [1])

The design of high lift systems is such that they are as simple as possible, but produce the required lift coefficient. A limiting factor is flow separation that occurs at moderate to high flap deflection angles, which limits the maximum achievable lift. Recent research in high lift systems has been focused on flow separation control in order to prevent separation on flaps, which allows a higher flap deflection angle. This increases the maximal achievable lift coefficient and might result in a smaller flap. It is

claimed that an improvement in the lift coefficient of 10% to 15% can be achieved by keeping the flow attached to the surface. A higher lift coefficient results in a lower minimum flight speed and therewith in a shorter required runway length [2, 3].

In recent years many active flow control actuators have been developed to postpone flow separation. In the current study the use of tangentially directed synthetic jets is considered.

In view of application to more efficient high lift systems, the focus is on flow separation control on the flap. To simplify the experiments, only the flap, represented by a common airfoil section, is studied.

1.1 Flow Control

In the same paper [4] in which in 1904 Prandtl proposed his boundary layer theory, he was the first to report on successfully influencing the boundary layer in order to alter the aerodynamic performance. This is called flow control. Flatt [5] offered in 1961 a definition for flow control (or boundary layer control):

"Boundary layer control includes any mechanism or process through which the boundary layer of a fluid flow is caused to behave differently than it normally would were the flow developing naturally along a smooth straight surface."

In the water tunnel experiments performed by Prandtl, flow separation in the flow over a circular cylinder is delayed by suction through a slot. This can be seen clearly in his flow visualization images, as displayed in Fig. 2 [4].

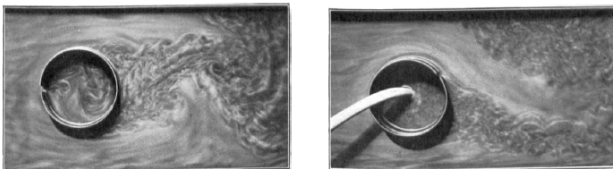


Fig. 2. Flow visualization of Prandtl's flow control experiments with no control (left); regular flow separation indicated by the vortical structures behind the circular cylinder, and flow control (right); separation delay on the upper side of the circular cylinder by suction through a slot at about the two o'clock position [4].

The flow control performed by Prandtl can be classified as flow separation control. The aim of this type of flow control is to delay flow separation. In case of airfoil flow with separation con-

trol, pressure drag is reduced, stall is delayed and lift is enhanced, because of improved pressure recovery. At high angles of attack, for which normally stall would appear, lift is still maintained, as illustrated in Fig. 3.

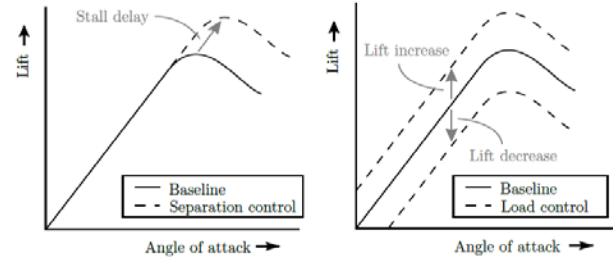


Fig. 3. Flow control: separation control (left) and load control (right).

Another large research area in flow control is the alteration of the streamlines around the airfoil such that the effective angle of attack is changed; this is called load control. Or, in other words, at the same angle of attack the lift is increased or decreased in a controlled manner, see Fig. 3.

Flow control can be achieved using both passive and active methods. Passive flow control is for example the application of vortex generators to influence turbulent boundary layer separation [6] or the air flow through the slots between the slat or flap and the main airplane wing [5]. In case of active flow control some kind of actuator is used to interact with the flow. The actuation of such a device can be predetermined, as was the case in Prandtl's experiments, or reactive. Then, sensors in combination with a feedback loop determine the level of actuation [7]. The focus of this paper is on predetermined active flow separation control.

Applications

Research is performed on many different applications of active flow separation control. An example is the drag reduction of the bluff body shape of a helicopter fuselage [8] or a generic ground vehicle [9]. Another example is flow separation control on turbine [10] and compressor blades [11] to increase their efficiency. Boeing investigated flow separation control on slats and flaps of high-lift multi-element wing sections to improve the aerodynamic performance at takeoff and landing [2]. At smaller scale research has been performed on the aerodynam-

ic improvement of micro-aerial vehicles [12]. Also investigated is flow separation control of wind turbine blades [13].

Methods

Separation occurs due to insufficient momentum in the boundary layer to counteract an adverse pressure gradient. Thus, adding momentum to the fluid in the boundary layer would delay separation. There are several methods to actively add more momentum to the boundary layer:

(i) Steady suction removes the low momentum boundary layer fluid next to the surface and attracts high momentum fluid from the free stream into the part of the boundary layer close to the wall. This makes the velocity profile fuller and the flow less inclined to separate. Prandtl [4] has used this principle in the experiments shown in Fig. 2.

(ii) Tangential blowing of high momentum fluid alters the velocity profile in the boundary layer such that it is more resistant to flow separation. The blowing can be done in a steady manner or in a periodic manner. The latter reduces the mass flow required for flow control.

(iii) Mixing of the high momentum free stream fluid with the low momentum boundary layer by generating large streamwise vortical structures. These structures can be created by periodic blowing in normal direction through holes in the surface. This is similar to the conventional passive vortex generators.

Combinations of above methods are also possible. An often used combination is periodically altering between blowing and suction such that net no mass flux occurs. Actuators which achieve this combination of blowing and suction are called Synthetic Jet Actuators or Zero Net Mass Flux actuators. In this paper the term Synthetic Jet Actuator (SJA) will be used.

The advantage of using SJA's is that an external source of fluid is not necessary to obtain the desired effect. For pulsed or steady blowing or suction, compressed air or a vacuum reservoir is required. The SJA uses the fluid flowing around the airfoil as source for the fluid ejected into the flow field. The SJA can be directed normal to the surface, creating streamwise vortical structures enhancing the mixing effect. Or it can be

directed tangentially, providing the effects of momentum addition by tangential blowing and removing the low momentum fluid in the boundary layer by suction. In the present paper SJA's will be utilized.

Synthetic Jet Actuators

Synthetic jets are typically formed by imposing a time periodic alternating pressure difference across an orifice, which produces a sequence of vortices. The pressure variation can be generated by a moving diaphragm or piston in a cavity connected to the surface through an orifice, see Fig. 4.

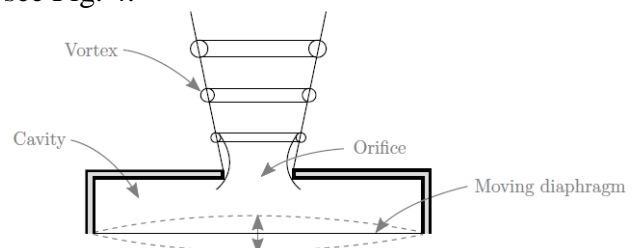


Fig. 4. Schematics of SJA.

During the upward motion of the diaphragm, the fluid in the cavity is pressurized, which causes an outflow through the orifice. In case of a normal directed SJA, the flow typically separates at the edge of the orifice, and a vortex sheet is formed which rolls up into a compact vortex that is advected away from the orifice under its own self-induced velocity. Fluid is sucked through the orifice into the cavity from all directions during the instroke, while during the outstroke the flow separates at the orifice edges and is blown in a specific direction. With this principle the synthetic jet adds momentum to the flow. At a certain distance from the orifice the effect due to the suction part of the cycle has disappeared. From this distance on the synthetic jet actually resembles a continuous jet [14].

1.2 Objectives Present Study

The present research is aimed at contributing to the knowledge in the field of flow separation control by performing experiments on a NACA0018 airfoil at high angles of attack. The method used to control the flow is periodic tangential blowing in combination with periodic

suction. This is realized by using synthetic jets directed tangential to the airfoil surface.

The orifice through which the synthetic jet is created will be a slit or a combination of slits along most of the span of the wing. In that way the results of the experiments can be compared with numerical simulations for 2D unsteady flow.

A final requirement is that the actuator used to generate the synthetic jet should be located inside the wing. This is different from earlier studies on load control at the University of Twente [15] in which large loudspeakers were mounted on both sides of the wing. One of the reasons for this requirement is to gain more control on the uniformity of the outflow of the synthetic jet.

2 Description Synthetic Jet Actuators

The piezoelectric actuator has recently become one of highly promising devices to produce the desired movement of the diaphragm in the cavity of SJA's. The primary advantages of piezoelectric transduction are low-power requirements, high bandwidth, and broadband output from DC to AC in the several kilo-Hertz range. [16]. Because of its simplicity, low mass and small size, in the current research the focus is on piezoelectric driven Synthetic Jet Actuators. Diaphragms with Piezo-electric elements have been widely applied in low-voltage sound devices like buzzers and speakers in mobile phones. These diaphragms are inexpensive (between 0.20€ and 2€), however, the displacement of the diaphragm is large enough for use in effective SJA's. Manufacturers typically recommend a maximum peak to peak input voltage of no more than approximately $15V_{pp}$. [17]. However, several studies [17, 18, 19] have shown that peak to peak voltages up to $200V_{pp}$ and $300V_{pp}$ can be applied without failure of the piezo element. Nevertheless, it might be possible that at these high voltages the piezo material depolarizes or degrades much faster than as specified by the manufacturer. For the short usage during experiments in a lab, this does not necessarily have to be a problem. A piezo element may be a so-called unimorphs, meaning

that it consists of one active layer piezo material and one inactive layer (shim). The performance of an element can be increased by applying parallel polarized piezo material on both sides of the shim, resulting in a so-called bimorph (two active layers).

An SJA can be characterized in terms of a number of parameters in order to quantify the performance of the SJA. Examples of these parameters are the momentum coefficient and the Velocity Ratio, based on the jet velocity.

2.1 Momentum Coefficient and Velocity Ratio

In the current research the aim of the SJA is adding momentum to the flow. This can be quantified by using a momentum coefficient. Unfortunately different definitions of the momentum coefficient are found in literature (see [17, 20, 21, 22, 23]). Most of these definitions, except the one from [17], do not employ the exact momentum that is transferred by the synthetic jet, but use some measure of the momentum. Most definitions use only the time-dependent centerline velocity at the jet exit plane or even only the peak jet velocity at the centerline; spatial variation in the velocity are not taken into account. The reason is the enormous amount of tests to be performed (in case of experimental research) in order to measure the time-dependent spatial distribution and then to calculate the momentum for all actuation parameters of interest. In the current research the spatial variation is neglected, as in the other studies, but the time variation of the velocity is taken into account. The momentum coefficient is defined as:

$$C_{\mu} = \frac{n_{sj} \bar{J}_{sj}}{\frac{1}{2} \rho_{\infty} U_{\infty}^2 A_w} \quad (1)$$

with $\frac{1}{2} \rho_{\infty} U_{\infty}^2$ the dynamic pressure of the free stream, A_w the wing reference area, n_{sj} the number of active synthetic jets and \bar{J}_{sj} the time-averaged momentum flux during the outstroke, defined as:

$$\bar{J}_{sj} = A_{sj} \frac{1}{\tau} \int_0^{\tau} \rho_{sj} u_j^2(t) dt \quad (2)$$

with τ the period of the jet outstroke, A_{sj} the surface area of a single synthetic jet orifice, ρ_{sj} the

density of the fluid in the jet and $u_j(t)$ the velocity on the centerline of the jet at the orifice exit. The orifice surface area is used instead of for example the slot width, in order to take into account the possible configurations like a number of separate slots, rather than a single slot along the whole span of the wing.

The density is assumed to be constant, because speeds higher than 0.2 times the Mach number are not expected. This makes the density time-independent, which means it can be taken out of the integral. The air inside the jet is assumed to have the density of the free stream ($\rho_{sj} = \rho_\infty$), rendering the momentum coefficient independent of the density.

A more simplified method to characterize the performance of an SJA is the Velocity Ratio, which is defined as the ratio between the maximum jet velocity during the outward stroke $u_{j,max}$ and the free stream velocity U_∞ .

$$VR = \frac{u_{j,max}}{U_\infty} \quad (3)$$

2.2 Helmholtz frequency

For a properly working SJA the internal dimensions of the actuator are important. The fluid inside the cavity can act as an acoustic spring and the fluid in the orifice as an acoustic mass. This mass-spring system has a resonance frequency, which is called the Helmholtz frequency. For inviscid, incompressible flow, the Helmholtz frequency is:

$$f_H = \frac{a}{2\pi} \sqrt{\frac{A_{sj}}{h_{eff} V}} \quad (4)$$

with a the speed of sound, A_{sj} the surface area of the orifice at the exit plane, h_{eff} the effective depth of the orifice and V the volume of the cavity. A so-called end-correction is required for h_{eff} similar to the effective mass in a mechanical spring-mass system.

For a circular cavity with a circular orifice this end correction is 1:7 times the radius of the orifice, which must be added to the geometric depth of the orifice. For other geometries, for example a rectangular orifice, estimating this end correction is not that obvious [24]. The Helmholtz frequency f_H together with the eigen-

frequency of the piezo diaphragm f_D determine the frequency response of the SJA. In case both frequencies are sufficiently far apart, they will be uncoupled. If these frequencies are closer together, coupling will occur, resulting in a single peak with a higher jet velocity than for the uncoupled case (see Fig. 5) [18].

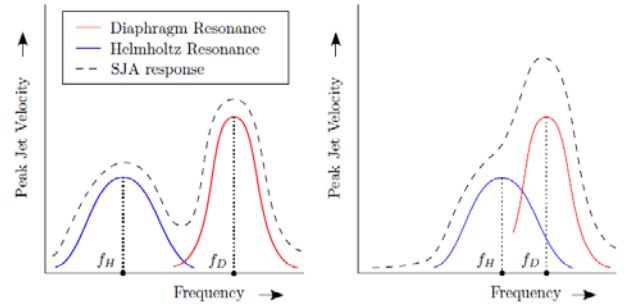


Fig. 5. Helmholtz and diaphragm mechanical resonance and overall SJA response. Uncoupled (left) and coupled (right) (adapted from [18]).

2.3 Actuation Frequency

The principle of the SJA is based on periodic blowing and suction. Therefore an important parameter to describe the performance of a Synthetic Jet Actuator is the Reduced Frequency F^+ . The actuation frequency is made non-dimensional with a characteristic length and a characteristic velocity. It relates the characteristic advection time over the separated flow domain with the period of the actuation cycle. In the current research, the dimensionless reduced frequency is based on the free-stream velocity U_∞ and the length of the separated flow region x_{te} .

$$F^+ = \frac{f_{act} x_{te}}{U_\infty} \quad (5)$$

Most research in the 80's and 90's in the field of flow separation control used a reduced frequency F^+ of $O(1)$. Actuation at these frequencies leads to the formation of vertical structures that scale with the length of the separated flow domain. The actuation frequency drives the shedding in the near wake. It is shown, however, that the lift fluctuates in the same frequency, resulting in alternating loads, which may be undesirable.

Glezer et al. [20] performed experiments with frequencies an order of magnitude higher than the shedding frequency ($F^+ \sim O(10)$). Their approach is based on altering the effective aerody-

dynamic shape of the airfoil instead of driving the vortex shedding. They showed that the resulting flow control was more effective and is effectively decoupled from the wake instability and, therefore, the modified aerodynamic forces tend to be virtually time-invariant [20].

2.4 Actuation Wave Form

The input signal to a piezo diaphragm used in flow control applications is periodic. The most straightforward periodic function is a sine, which is also the most used waveform in flow control. Mane et al. [25] considered different waveforms, like a square and a saw tooth driving signal, in order to achieve a maximum peak jet velocity. They showed that the sawtooth and square signal produced a significantly higher peak jet velocity compared to the one produced using the sine function. However, the velocity output appears to be much more chaotic. This means that, although the sawtooth and square waveform have a higher peak jet velocity, in terms of addition of momentum as function of time, the sine may perform better. In the present study the sine wave form is used.

2.5 Location Actuator

For a proper functioning of flow separation control, the location of the SJA is of great importance. In order for the actuator to be effective, it should be placed upstream of the location of separation. The most effective location is closest to the separation point. Duvigneau et al. [26] determined numerically the best location of the SJA in order to increase the time-averaged lift for a NACA0012 airfoil at an angle of attack of 18 deg. At a Reynolds number of 2×10^6 this location was found to be at 23% chord.

This corresponds approximately with the location of separation of 21% chord found employing RFOIL (version (1.1) [27]. RFOIL is similar to XFOIL [28], but with an improved prediction of 2D post-stall lift (see [29]), as required for predicting more accurately the stall of wind turbine airfoil sections. XFOIL is known to over

predict the stall angle and corresponding lift coefficient.

The input parameters for RFOIL were: 200 panels; $Re = 2 \times 10^6$; $M = 0.07$; $\alpha = 18$ deg; $x_{tr,upper}/c = 0.03$; $x_{tr,lower}/c = 0.10$; turbulence intensity 0.07% ($N_{crit} = 9$).

The goal of flow separation control is to keep the flow attached also at higher angles of attack for which without actuation stall would occur. This means that the SJA must be positioned upstream of the point of flow separation in stall. For the NACA0018 airfoil section this was determined as 64% chord and 49% chord with RFOIL and XFOIL, respectively.

2.6 Geometry Orifice

The geometry of the orifice is important for the Helmholtz frequency, but it also influences the formation of the vortical structures that form the synthetic jet. There have been a number of studies on the generation and evolution of synthetic jets emitting from circular and rectangular exits in the direction normal to the surface, e.g. Minhee Kim et al. [30]. However, in the present study we have chosen to consider tangential blowing for flow separation control. The Coandă effect will help to direct the flow from the slot along a mildly curved surface in the direction tangential to the surface.

This leads to the choice of rectangular orifices with a large aspect ratio.

2.7 SJA with slotted orifice

Most piezo-electrically driven synthetic jet actuators found in literature, that are manufactured for experimental research, do have circular orifices, like [18, 19, 25]. Six actuators have been found in literature with rectangular orifices; Oyarzun and Cattafesta [17], Yang [31], Kim and Garry [32], Mossi and Bryant [33], Amitay and Glezer [34], Vasile and Amitay [35]. These six will be discussed in this section. Oyarzun [17] optimized the cavity and orifice dimensions for a given piezo disk and predefined constraints. The optimized result has been manufactured and experimentally tested to verify the numerical si-

mulation. Yang [31] designed a dual-diaphragm synthetic jet actuator to experimentally analyze the flow generated by this device using PIV measurements. The results of these experiments are then compared with results of numerical simulations. Kim [32] designed a modular SJA with a rectangular orifice to study the effect of varying the orifice aspect ratio as well as the cavity depth. Mossi [33] used three types of custom fabricated piezo elements to characterize the relevant properties for the design of a synthetic jet. Amitay [34] performed flow control experiments for a modified unconventional airfoil using piezo-electrically driven synthetic jet actuators. Vasile [35] carried out flow control experiments for a finite and for a swept-back wing. In a rectangular domain stereoscopic PIV measurements were performed to get insight in the flow structures around the synthetic jet. The properties of a number of synthetic jet actuators with a slotted orifice are listed in Table 1.

	Oyarzun[17]	Yang[31]	Kim[32]	Mossi[33]
Maximum centerline jet				
velocity u_j (m/s)	53.6	30.1	7	4.5
Actuation voltage E_{act} (V _{pp})	100	45	30 – 50	400
Actuation frequency f_{act} (Hz)	700	648	300 – 4000	5
Piezo diaphragm(s)	Sound component	Custom fabricated	Sound component	Custom fabricated
No. of active layers per diaphragm	Bimorph	Unimorph	Unimorph	Unimorph / Bimorph
Diaphragm configuration	Single	Dual	Single	Single
Diaphragm diameter (mm)	37	50	23	63.5
Cavity volume (m ³)	$4.47 \cdot 10^{-6}$	$9.82 \cdot 10^{-6}$	$1.16 \cdot 10^{-7}$ – $1.15 \cdot 10^{-6}$?
Orifice dimensions				
Orifice width (mm)	0.5	0.5	0.28	0.52
Orifice length (mm)	30	35	2 – 22	34.9
Orifice depth (mm)	1.5	?	6.5	?
Orifice configuration	Adjacent	Adjacent	Adjacent	Opposite
Waveform	Sine	Sine	Square	Sine / Square / Saw tooth

Table 1. Synthetic jet actuators from literature

Unfortunately, not much is known about the actuators from Amitay and Vasile. Therefore they are not listed in the table. From the actuator of Amitay it is known that it is actuated at frequencies of 740, 1088 and 1480 Hz, that it has a high aspect ratio rectangular 140 mm by 0.5 mm orifice, but the jet velocities that can be generated are not known. The actuator of Vasile has a 1 mm by 19 mm slot and is actuated at a frequency of 1700 Hz, which results in a time-averaged jet velocity of 14 m/s.

From the actuators listed in Table 1 only two actuators are able to generate a reasonable jet velocity; these are designs by Oyarzun and by Yang. These two designs have similarities in terms of actuation frequency, orifice dimensions, orifice configuration and waveform. Both designs have two active piezo layers within the actuator, although Oyarzun's actuator contains one diaphragm with two piezo layers (bimorph) and Yang's actuator two diaphragms with each one piezo layer (unimorph).

Because of a smaller diaphragm diameter, the actuator designed by Oyarzun is smaller compared to the actuator designed by Yang. Also, the cavity volume is approximately half the size of the one from Yang. Another difference is the used piezo diaphragm; Oyarzun used "cheap" sound components, whereas Yang used more expensive custom manufactured ones.

For the present study the design of Oyarzun has been selected as the basis for the design of an SJA that has the potential to produce an adequate jet velocity, is small enough to be mounted inside the available wind-tunnel model, while its piezo diaphragm is not too expensive.

3 Design and Test of SJA

The optimized parameters for an actuator developed by Oyarzun and Cattafesta [17] at the University of Florida are used as input for the design of an actuator for the present research. Oyarzun used Lumped Element Modeling (LEM) to perform a constrained design optimization of actuators of various topologies. One of these cases optimizes an actuator with a given piezoceramic diaphragm (P412013T-JB of APC International Ltd.), with a 37 mm clamp diameter, and a fixed slot length of 30 mm. The design variables, orifice width, orifice height and cavity volume are optimized within predefined constraints. The results are listed in Table 2.

Clamp diameter diaphragm, d_{clamp} :	37 mm
Orifice length, l :	30 mm
Orifice width, w :	0.5 mm
Orifice height, h :	1.5 mm
Cavity volume, V :	$4.47 \times 10^{-6} \text{ m}^3$

Table 2. Parameters of optimized SJA of Oyarzun [17]

The cavity volume V and the orifice height h are between the predefined upper and lower bounds of the optimization. The orifice width w , however, is situated on the lower bound, which is 0.5 mm. This means that the real optimum might be located at a still lower value of the orifice width.

For the optimized parameters, listed in Table 2 the actuator outputs the highest jet velocity, which is approximately 54 m/s, at 700 Hz. According to Oyarzun, the diaphragm natural frequency is 750 Hz and the Helmholtz frequency of the cavity in combination with the orifice is 1267 Hz. These frequencies are thus quite far apart, meaning that coupling cannot occur, which might have given the jet velocity an additional boost (see Fig. 2).

3.1 Present Design of SJA

In the current research it has been attempted to improve the performance of the actuator by halving the width of the orifice from $w = 0.5$ mm to $w = 0.25$ mm. This has three advantages:

- (i) Reducing the orifice surface area, for the same volume displacement, results in a higher jet velocity;
- (ii) Based on Eq. (4) for the Helmholtz frequency, reducing the orifice width will reduce the Helmholtz frequency. By halving the orifice width the Helmholtz frequency will reduce to a value close the diaphragm eigenfrequency. The coupling of these frequencies may then result in a higher jet velocity.
- (iii) In the actuator's flow separation control application the orifice is oriented tangential to the airfoil surface. A smaller orifice will result in a smaller disturbance of the flow over the wing.

Geometry Actuator

The design of the Synthetic Jet Actuator used in the preliminary experiments consists of seven parts. An exploded view of the actuator is displayed in Fig. 6. A photograph of the assembled actuator is presented in Fig. 7.

The piezo diaphragm is a bimorph sound component with part number P412013T-JB manufactured by APC International, Ltd.

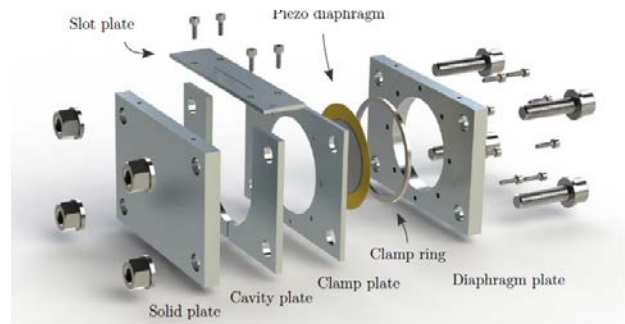


Fig. 6. Exploded view of SJA used in test set-up

This is the same diaphragm as used in the actuator Oyarzun [17]. The diaphragm consists out of a 0.1 mm thick brass plate with a diameter of 41 mm with on both sides a 0.15 mm thick piezo ceramic disk with a diameter of 29 mm. The slot plate contains a slot that is 30 mm long and 0.25 mm wide. Two slot plates have been manufactured: one with the slot located in the middle of the cavity plate, similar to Oyarzun [17]; and one with the slot located flush with the solid plate (see Fig. 6). The latter geometry is similar to the geometry of the actuators placed in the wing with tangential blowing. Further details of the design and manufacturing of the SJA can be found in [36].



Fig. 7. Photograph of SJA used in test set-up

Actuation

The actuation setup used for the measurements of the displacement and jet velocity is as follows. A sinusoidal signal is generated using a GW Instek SFG-2110 synthesized function generator amplified to the desired voltage with a RMX 2450 power amplifier from QSC. In order to prevent peak voltages the piezo element is connected in series with a (100 Ω , 1 W) resistor. The voltage over the piezo element is measured with a PeakTech 3720 DMM digital multimeter

Diaphragm Displacement

The displacement of the center of the piezo element clamped in the actuator has been measured, inside an acoustic room, using an accelerometer (Brüel & Kjær Type 4374).

Fig. 8 shows for $E_{act} = 100 V_{pp}$, the results for the amplitude of the displacement as a function of actuation frequency. The largest displacement is obtained at an actuation frequency of 1000 Hz and is equal to about 0.31 mm. At lower frequencies the maximal displacement asymptotically decreases towards a displacement equal to the displacement obtained when applying a constant voltage of 100 V. At a frequency of 750 Hz a local extra increase in the displacement amplitude is observed. This is presumably caused by the eigenfrequency of the piezo diaphragm, which is equal to 750 Hz as Oyarzun [17] reported. For actuation frequencies above 1000 Hz the displacement of the center of the piezo diaphragm rapidly decreases to almost zero. This is because at these frequencies the second mode of the piezo diaphragm is excited. In this mode the center of the piezo diaphragm is a node. Although the center of the piezo diaphragm is not moving, the volume is still varying, which still might generate a synthetic jet.

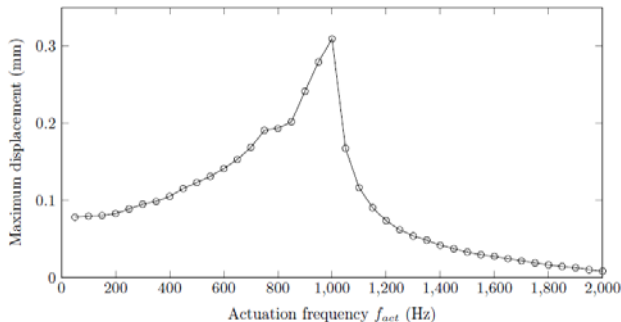


Fig. 8. Amplitude displacement center of piezo diaphragm as function of actuation frequency. $E_{act} = 100 V_{pp}$.

Increasing the actuation voltage, at $f_{act} = 700$ Hz, increases the amplitude of the displacement of the center of the diaphragm in a linear fashion, up to $E_{act} = 200 V_{pp}$.

3.2 Performance of SJA

The jet velocity is measured using a (1D) hot-wire system (Dantec probe 55P11). The hot-wire

is positioned as close as possible to the slot, at approximately an angle of 45 degrees with respect to the actuator surface (see Fig. 9).

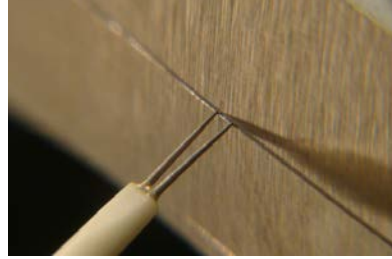


Fig. 9. Positioning of hot wire at an angle of 45 deg with respect to actuator surface.

The sample frequency is set such that for each actuation frequency one period of blowing and suction consists of 200 sample points.

Induced Velocity during Single Cycle

A typical velocity signal during a single period, measured at the centerline of the slot, is presented in Fig. 10.

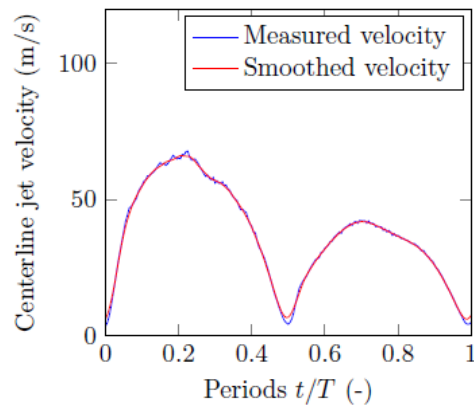


Fig. 10. Measured magnitude of the centerline velocity during one period ($f_{act} = 900$ Hz, $E_{act} = 100 V_{pp}$)

The first half of the signal represents the blowing phase of the period; the second half the suction phase. The 1D hot-wire measures the magnitude of the velocity and not its direction. Therefore the signal of both the blowing and suction phase is positive. Since the SJA is a zero-net-mass-flux actuator, the outward component of the blowing and the inward component of the suction velocity should be of the same magnitude. However, because the hot-wire is not placed inside the slot, but a very small distance above the slot (see Fig. 9), the measured magnitude of the velocity during the suction phase is lower. Here only the blowing velocity will be considered.

Maximum Induced Velocity vs Frequency

Fig. 11 presents the results of the maximum centerline jet velocity as function of the actuation frequency for the present design with the actuator as well as for the design of Oyarzun [17]. For most frequencies the present design with $w = 0.25$ mm width of the slot indeed produces higher velocities than the design of Oyarzun with $w = 0.5$ mm. The jet velocity is higher, because the slot area of the present actuator is half that of Oyarzun's. This has two effects. With the same volume displacement generated by the piezo element, a higher jet velocity is required to transport the same amount of air through the smaller slot. The second effect is that the Helmholtz frequency of the cavity and slot, which equals 1267 Hz, is reduced to a value closer to the diaphragm eigenfrequency of 750 Hz.

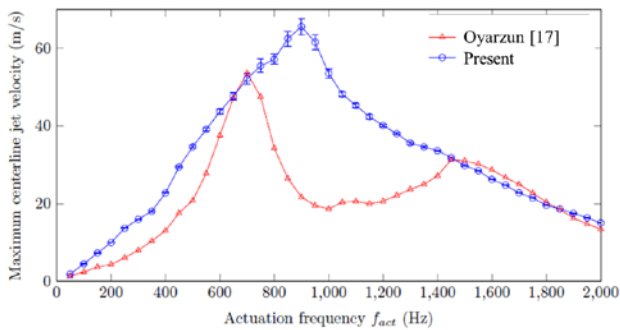


Fig. 11. Comparison of maximum centerline outstroke jet velocity as function of actuation frequency of design of [17] ($w = 0.5$ mm) and present design ($w = 0.25$ mm). $E_{act} = 100 V_{pp}$.

For Oyarzun's design this results in two peaks in the jet velocity response, as seen in Fig. 11. The Helmholtz frequency of the present actuator is closer to the diaphragm eigenfrequency so that coupling between the frequencies occurs.

For the present actuator the optimal actuation frequency for generating the highest jet velocity is 900 Hz. At this frequency the actuator produces a jet with a maximum outstroke velocity of 65.5 m/s. This is 22% higher than the velocity generated by the actuator design of Oyarzun [17] at its optimal actuation frequency of 700 Hz. From Fig. 11 it can be observed that for a higher jet velocity the variation in the maxima determined over 100 periods becomes larger.

Maximum Induced Velocity vs Voltage

In Fig. 12 the maximum centerline jet velocity of the actuator is presented as function of the actuation voltage. Results are given for $f_{act} = 700$ Hz and for $f_{act} = 900$ Hz, which is the frequency for which the highest maximum jet velocity is measured.

The maximum actuation voltage that the amplifier can produce is $200 V_{pp}$ for $f_{act} = 700$ Hz and $190 V_{pp}$ at $f_{act} = 900$ Hz. This is because the piezo diaphragm works as a capacitor, i.e. the impedance of the piezo disk decreases with increasing actuation frequency, requiring at the same voltage more power from the amplifier.

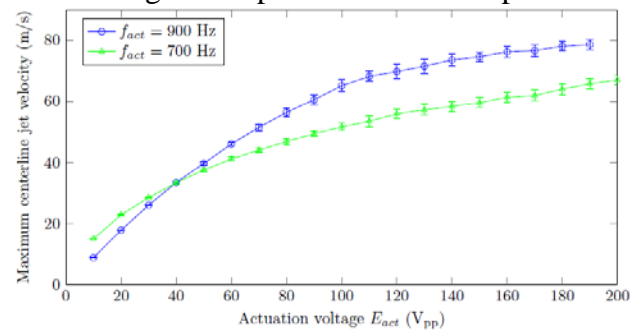


Fig. 12. Maximum centerline jet velocity as function of actuation voltage. $f_{act} = 700$ Hz and 900 Hz.

Although it was found that the displacement of the center of the piezo diaphragm increases about linear with actuation voltage, the jet velocity, increases less than linear with voltage. It is assumed that this is caused by non-linear flow effects inside the cavity. Almost doubling, at an actuation frequency of 900 Hz, the actuation voltage (from $100 V_{pp}$ to $190 V_{pp}$), increases the maximum centerline jet velocity with approximately 20% only. This means that doubling the displacement does not result in a jet velocity that is twice as large. This is in agreement with a numerical study performed by the Fraunhofer ENAS and the Chemnitz University of Technology [37] indicating that a dual diaphragm actuator does not generate a two times higher jet velocity.

Centric or Eccentric Orifice

Comparison of the results obtained for the SJA with centric orifice and the ones for the SJA with eccentric orifice have shown that the eccentric orifice produces a lower jet velocity. The maximum centerline jet velocity for the SJA

with eccentric orifice is 9.6 % lower than that generated by the centric orifice at an actuation frequency of 900 Hz and a actuation voltage of 100 V_{pp}.

4 Design Wing with Flow Separation Control

Flow separation control experiments have been performed for a 2D wing with a NACA0018 section. Actuation is performed using ten Synthetic Jet Actuators, which have the internal dimensions of the SJA described in section 4. The SJA's have the eccentric slot described in section 3. Fig. 13 gives a schematic drawing of the airfoil containing the cavity and slot.

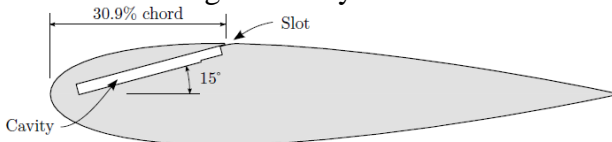


Fig. 13. Schematic drawing of airfoil section with cavity and slot (drawing is to scale).

4.1 Design

The slots are located in the upper surface of the airfoil at 51 mm from the leading edge, i.e. at 30.9% chord. This is the location closest to the leading edge possible with this actuator with the slot still aligned with the cavity solid plate, see Fig. 6. This is also the location where the flow separates according to RFOIL for an angle of attack of 17 deg, whereas the stall angle is slightly higher than 13 deg. This suggests that when blowing from this location flow separation control can be achieved up to an angle of attack of about 17 deg.

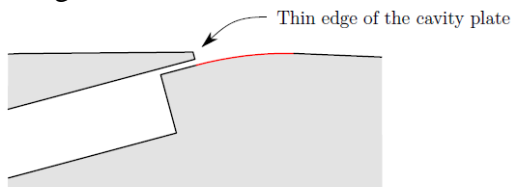


Fig. 14. Close up of slot. In red the rounding of the external edge enabling Coandă effect (drawing is to scale).

The actuator is placed at an angle of 15 deg with the chord line, which corresponds with an angle of 15.35 deg between the slot exit and the airfoil's upper surface. The jet will be directed tangential to the airfoil surface by the Coandă ef-

fect by rounding the lower external edge, see Fig. 14. The rounding consists of a circular arc with a radius of 14.05 mm.

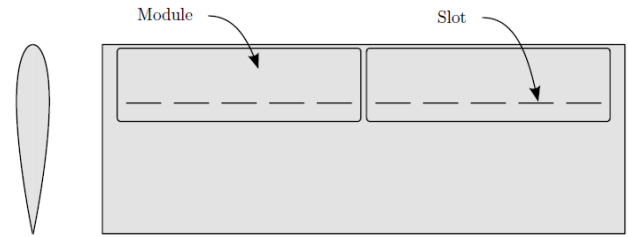


Fig. 15. Top view of wing with two modules with five slotted SJA's each (drawing isto scale)

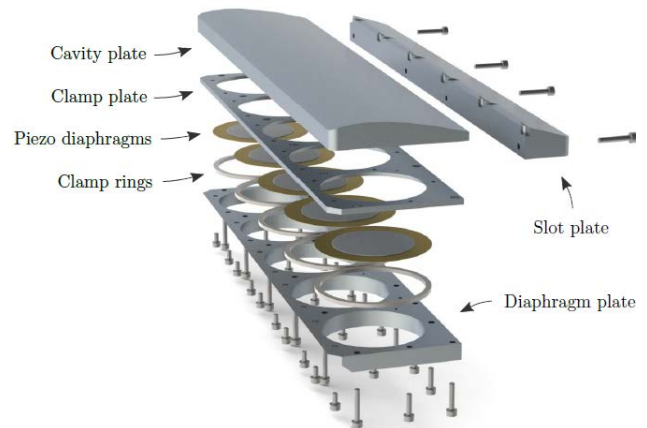


Fig. 16. Exploded view of single module with five SJA's

4.2 Placement SJA's

The actuators are placed in two modules, each with five actuators, see Fig. 15. In case a piezo disk has to be replaced, only part of the set-up has to be disassembled. Furthermore, the wing remains stiffer because of the rib between the two modules. The 30 mm long slots of the SJA's in the two modules cover about 66% of the wing's 0.455 m span. A module consists of six parts; cavity plate, clamp plate, piezo diaphragm, clamp ring, diaphragm plate and slot plate, see Fig. 16. Fig. 17 shows the installed SJA inside the airfoil.

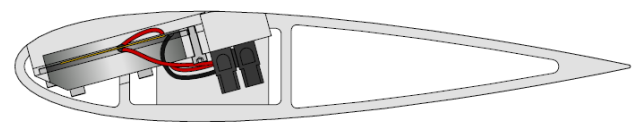


Fig. 17. Cross-section airfoil with SJA

4.3 Actuation

The setup for actuation of the ten piezo elements is the same as used for the single actuator in section 3. Instead of one switch, one resistor and one piezo element, now ten switches, ten 100 Ω resistors and ten piezo elements are connected in parallel. The voltage is still measured over one piezo element. Ten switches are used such that the piezo elements can be turned on and off individually. In that way prior to every measurement campaign it can be checked whether all piezo element operate.

Because of the high resistance of the piezo elements and a ten times larger current compared to the single actuator, the amplifier can only supply at its maximum an actuation voltage of 100 V_{pp} . However, that is sufficient for the present study.

5 Wind Tunnel Experiments

Experiments have been performed using the 11 kW wind tunnel facility from the University of Twente, see Fig. 18

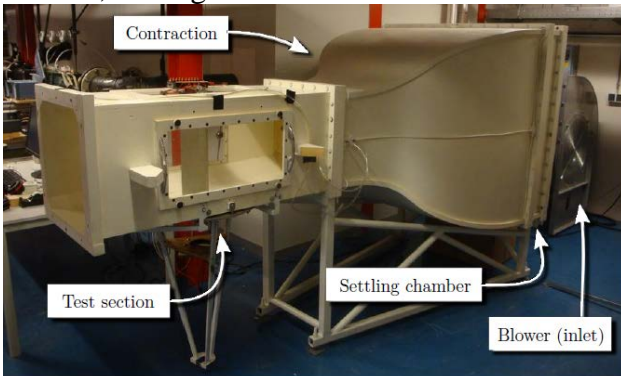


Fig. 18. The 11 kW wind tunnel of the University of Twente.

The wind tunnel is an open return tunnel with a closed test section, which has a cross section of 0.455 m by 0.455 m.

The maximum velocity the tunnel can achieve is 25 m/s. The turbulence level $I = |\overline{u'}|/U_\infty$ is 2%. This turbulence level is rather high. Wind tunnels designed for low turbulence measurements typically have turbulence levels lower than 0.3%.

All experiments have been performed at a fixed free stream velocity of 25 m/s, which, with a chord of the NACA0018 section of 0.165 m, results in a chord Reynolds number of 2.73×10^5 . Most flow control experiments have been performed for a clean airfoil (no turbulators applied to trip the boundary layer). However, some experiments have been performed with turbulators in order to eliminate the laminar separation bubble and generate a flow that is more representative of that over the flap of an aircraft wing.

The dimensionless numbers F^+ (Eq. 5) and VR (Eq. 3) are based on the jet velocity produced by the actuator as measured for a single isolated actuator with the eccentric slot, see section 3. The actuation frequency and jet velocity are made dimensionless as described in section 3 using the free stream velocity of $U_\infty = 25$ m/s and the maximum length of the separated flow region $x_{re} = 0.114$ m. The results for the isolated SJA are displayed in Fig. 19 and Fig. 20.

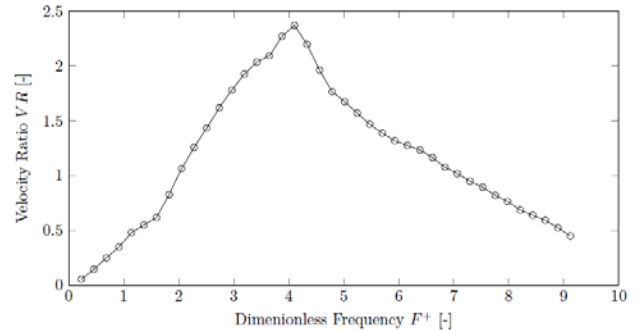


Fig. 19. Velocity Ratio VR as function of the dimensionless frequency F^+ at actuation voltage of 100 V_{pp} for SJA with eccentric slot.

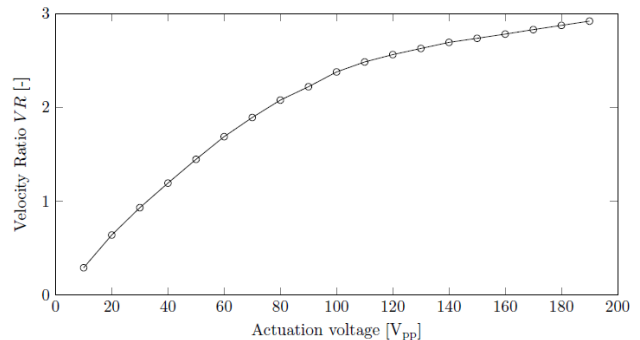


Fig. 20. Velocity Ratio VR as function of actuation voltage at an actuation frequency of 900 Hz ($F^+ = 4.1$) for SJA with eccentric slot.

The jet velocities produced by the tangential jets in the airfoil have not been measured yet. For the present study it is assumed that the jet veloc-

ity of the actuators in the airfoil do not differ much from that of the isolated actuator with the eccentric slot, because of their geometric similarity.

5.1 Clean Wing without Actuation

The lift force on the 2D wing has been measured first without actuation. This data serves as a reference value for the flow control measurements. This setup is referred to as "clean". The effect of the slots on the lift curve is determined by comparing the results for the case that the slots are taped with the results for the case with open slots but without actuation, see Fig. 21. No significant difference is observed.

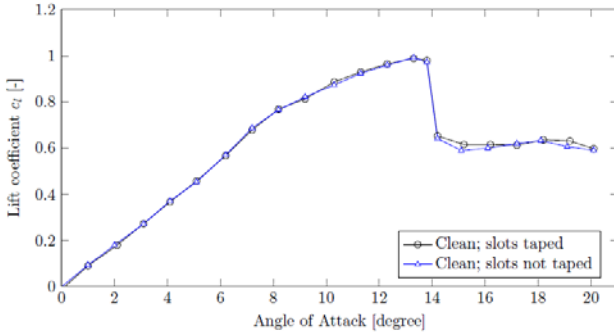


Fig. 21. Lift curve for NACA0018 airfoil with taped slots compared with lift curve for case without actuation with open slots ($Re_c = 2.73 \times 10^5$, $Ma_\infty = 0.07$).

The lift curve measured in the present research has been compared with measurement data from Timmer [38] at the approximately the same Reynolds number (3×10^5).

At low angles of attack (below 6 deg) the two measurements show the same linear trend with $\alpha_{L=0} = 0$ and a slope of about 2π , the values from thin-airfoil theory. At high angle of attack for which stall occurs the trend of the data in the present research is similar to Timmer's data; this trend in stall is called abrupt stall. However, Timmer found a significant higher stall angle of 17 deg, compared to 13.5 deg in Fig. 21, though the maximum lift coefficient does not differ much.

5.2 Clean Wing with Actuation

Effects of jet velocity VR

Measurements have been performed at a fixed frequency of $F^+ = 4.1$ at varying actuation voltages. This frequency of 900 Hz is chosen because at this frequency the isolated SJA produces the highest jet velocity. For the jet velocity the values $VR = 1, 1.5, 2$ and 2.4 have been selected. Fig. 22 shows the resulting lift curves for angles of attack higher than 8 degrees. From this figure it is clear that the tangentially directed synthetic jet indeed is able to perform flow separation control. At the dimensionless actuation frequency of 4.1 a higher jet velocity results in better performance in terms of higher stall angle and higher maximum lift coefficient. At the highest jet velocity ratio of $VR = 2.4$ the stall angle is increased by 18.1% and the maximum lift coefficient by 12.9% compared to the values without actuation.

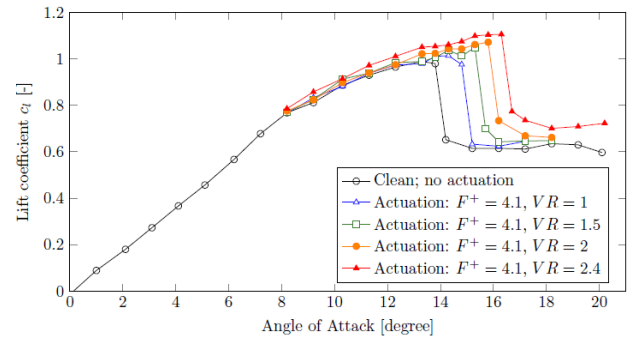


Fig. 22. Effect of jet velocity on performance of SJA flow separation control. Clean NACA0018 wing ($F^+ = 4.1$, E_{act} based on Fig. 20, $Re_c = 2.73 \times 10^5$, $Ma_\infty = 0.07$).

Effects of actuation frequency F^+

At a fixed velocity ratio of $VR = 1.44$ measurements have been performed at dimensionless frequency of $F^+ = 2.5, 4.1$ and 5.5 ($f_{act} = 550$ Hz, 900 Hz and 1200 Hz). The resulting lift curves are presented in Fig. 23.

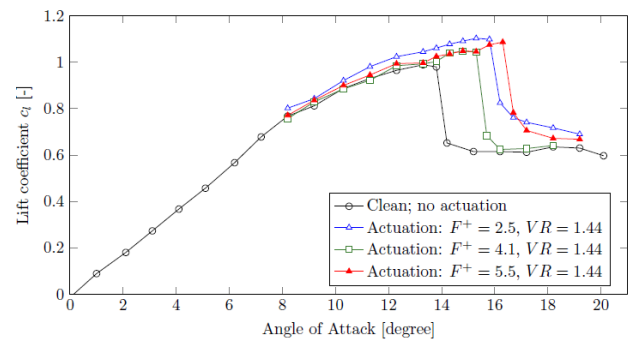


Fig. 23. Effect of actuation frequency F^+ on performance of SJA flow separation control. Clean NACA0018 wing ($VR = 1.44$, E_{act} based on Figs. 19 and 20, $Re_c = 2.73 \times 10^5$, $Ma_\infty = 0.07$).

From Fig. 23 it can be seen that the frequency at which the effect of the jet velocity was examined ($F^+ = 4.1$) in Fig. 22 shows the poorest flow control performance. At the lower F^+ of 2.5 the flow control performs best in terms of increase in maximum lift coefficient. At the higher F^+ of 5.5 the flow control performs best in terms of increase in stall angle.

Optimal set of actuation parameters

Based on the results for the effect of the jet locity, it can be concluded that a higher jet velocity results in a better flow control performance. Therefore the best actuation voltage is the maximum voltage that the amplifier can generate, which is in the present case $E_{act} = 100 V_{pp}$. The jet velocity produced by the actuator at this voltage depends on the actuation frequency. The corresponding velocity ratio follows from Fig. 19. At the actuation voltage of $100 V_{pp}$ the actuation frequency is varied for three angles of attack: 16, 17 and 18 deg, see Fig. 24.

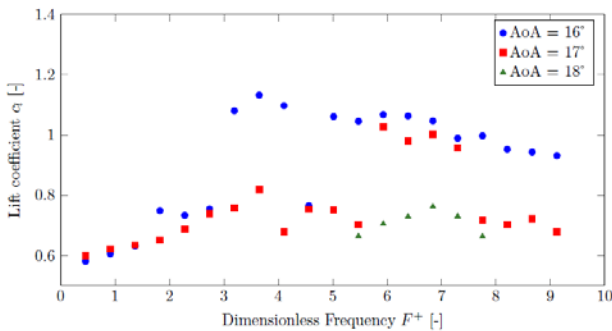


Fig. 24. Lift coefficient for $\alpha = 16, 17$ and 18 deg as function of dimensionless actuation frequency F^+ at the maximal actuation voltage of $E_{act} = 100 V_{pp}$ ($Re_c = 2.73 \times 10^5$, $Ma_c = 0.07$).

This figure shows that for an angle of attack of 16 deg for a wide range of actuation voltages flow separation is delayed and a lift coefficient of around 1.0 is produced. Even for the highest F^+ of 9.1, corresponding with a velocity ratio of only 0.5 (see Fig. 19), this is achieved. For this angle of attack actuation at an F^+ lower than 3.0 is insufficient to delay flow separation.

At an angle of attack of 17 deg, only for dimensionless frequencies between 5.9 and 7.3 stall can be prevented. This is remarkable, because for lower dimensionless frequencies, as low as 2.5 a twice higher jet velocity is generated by the actuator (see Fig. 19). This implies that for

flow separation control frequency is of greater importance than jet velocity.

At an angle of attack of 18 deg, also for frequencies of F^+ between 5.9 and 7.3 the actuator is not able to prevent stall.

Considering the most important effect of flow separation control to be the increase of the stall angle, an F^+ between 5.9 and 7.3 performs best for all angles of attack. Within this range the actuation at $F^+ = 5.9$ produces the highest lift coefficient, probably due to the higher jet velocity at this frequency. The lift curve for this set of actuation parameters, $F^+ = 5.9$ and $E_{act} = 100 V_{pp}$ (resulting in a VR of 1.32), is presented in Fig. 25.

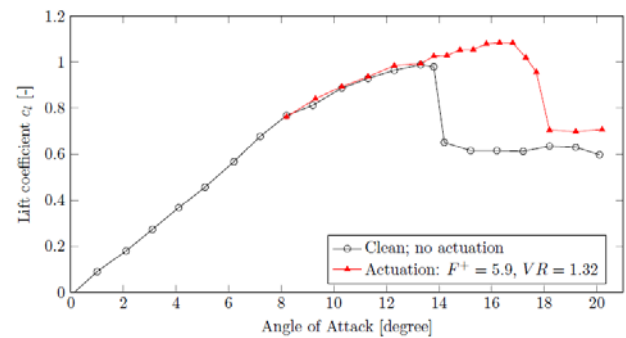


Fig. 26 Flow separation control for clean NACA0018 wing using optimal set of parameters for the present SJA: $F^+ = 5.9$ and $E_{act} = 100 V_{pp}$ ($Re_c = 2.73 \times 10^5$, $Ma_c = 0.07$).

Using the optimal set of parameters the stall angle is increased by 22% to a value of 16.8 deg and the maximum lift coefficient is increased by 11% to a value of 1.08.

5.3 Wing with Turbulators and Actuation

The Reynolds number at which the above flow control experiments have been performed is much lower than the Reynolds number relevant for the flow over flaps of aircraft wings, for which flow separation control might be applied. In order to generate a flow which is in the same flow regime as flows at higher Reynolds numbers, turbulators are used. These turbulators fix the location on the airfoil where transition from laminar to turbulent flow takes place. The turbulator will prevent the formation of the laminar separation bubble, which is present for the Rey-

nolds number at which the measurements have been performed.

The turbulator applied is the Streifender turbulator strip with thickness of 0.4 mm, width of 6 mm, zig-zag angle of 70 deg, placed at 4 % chord.

Flow separation control is applied to the wing with the turbulator strips. The parameters of the actuation are set such that the jet velocity of the actuator is the highest; these are: $F^+ = 4.1$ and $VR = 2.4$, see Fig. 19. The resulting lift curve is presented in Fig. 27.

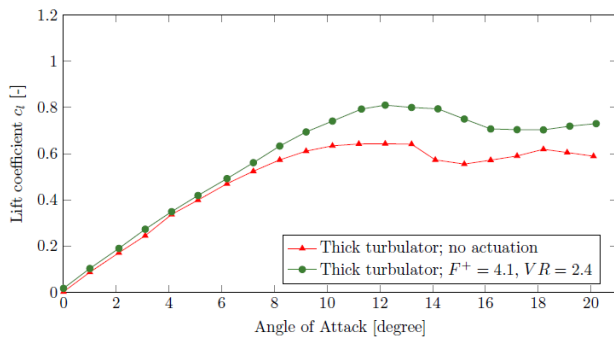


Fig. 27. Flow separation control for tripped NACA0018 wing with turbulator strips at 4% chord on both sides wing ($F^+ = 4.1$, $E_{act} = 100 V_{pp}$, $VR = 2.4$; $Re_c = 2.73 \times 10^5$, $Ma_\infty = 0.07$).

By performing actuation the maximum lift coefficient increases by 26% from 0.64 to 0.81. However, no clear change in stall angle can be observed.

6 Conclusions

A synthetic jet actuator with a slotted orifice has successfully been designed and manufactured. The SJA has dimensions such that it fits in a NACA0018 airfoil with 0.165 m chord. The design is based on a design by the University of Florida [17]. The performance of the actuator is improved by reducing the slot width from 0.5 mm to 0.25 mm. For the present design the maximum outstroke jet velocity is 65 m/s applying an actuation voltage of $E_{act} = 100 V_{pp}$, at the SJA's optimum actuation frequency of $f_{act} = 900$ Hz, compared to 53 m/s at $f_{act} = 700$ Hz for the design of the University of Florida.

For the purpose of flow separation control an experimental setup has successfully been designed and manufactured. This set-up contains

ten SJA's placed in a 2D NACA0018 wing with a span of 0.45 m. The slots of the ten SJA's cover about 66% of the span of the wing. During outstroke the jet of the actuator exits tangentially to the airfoil upper surface utilizing Coandă's effect. During instroke the actuator inhales the low momentum fluid in the boundary layer.

The location of the slot at 30.9% chord has been chosen in order to enable flow separation control to delay flow separation that without control occurs at an angle of attack between 16 and 17 deg, whereas the stall angle is around 13 deg. Wind tunnel experiments have been performed measuring the lift force acting on the airfoil, both with and without actuation. The conditions correspond to $Re_c = 2.73 \times 10^5$, $Ma_\infty = 0.07$. By varying the actuation voltage the jet velocity is varied between 1 and 2.4 times the free stream velocity at a fixed actuation frequency of $F^+ = 4.1$ ($f_{act} = 900$ Hz). It turned out that for a higher jet velocity the stall angle is increased while also the maximum lift coefficient is increased.

Varying the actuation frequency between $F^+ = 2.5$ and 5.5 at a fixed jet velocity of $VR = 1.44$ showed that the actuation frequency has a large effect on flow separation control performance. Both the lower and higher actuation frequency performed better than the actuation frequency at which the jet velocity had been varied ($F^+ = 4.1$).

The actuation frequency at which the present actuator has the best flow separation control performance (at its maximum actuation voltage of $E_{act} = 100 V_{pp}$) has been determined to be $F^+ = 5.9$. At this frequency and voltage the actuator produces a maximum jet velocity of 1.32 times the free stream velocity. With these optimal parameters the stall angle is increased by 22% to a value of 16.8 degrees and the maximum lift coefficient by 11% to a value of 1.08.

References

- [1] Höll T, Wassen E and Thiele F. Active separation control on a high-lift configuration using segmented actuation slots. *Proc. 5th AIAA Flow Control Conference*, Chicago, Illinois, USA, AIAA Paper 2010-4249, 2010.

- [2] Shmilovich A and Yadlin Y. Active flow control for practical high-lift systems. *Journal of Aircraft*, Vol. 46, No. 4, July-August 2009.
- [3] Petz R and Nitsche W. Active control of flow separation on a swept constant chord half model in a high-lift configuration. *Proc. 3rd AIAA Flow Control Conference*, San Francisco, California, USA, AIAA Paper 2006-3505, 2006.
- [4] Prandtl L. Über Flüssigkeitsbewegung bei sehr kleiner Reibung. III Internationalen Mathematiker-Kongresses, Heidelberg, Germany, 1904.
- [5] Gad-el-Hak M. *Flow Control; Passive, Active, and Reactive Flow Management*. Cambridge University Press, 2000.
- [6] Gallas Q, Holman R, Raju R and Mittal R. Low dimensional modeling of zero-net mass-flux actuators. *Proc. 2nd AIAA Flow Control Conference*, Portland, Oregon, USA, AIAA Paper 2004-2413, 2004.
- [7] Tian Y, Song Q and Cattafesta L. Adaptive feedback control of flow separation. *Proc. 3rd AIAA Flow Control Conference*, San Francisco, California, USA, AIAA Paper 2006-3016, 2006.
- [8] Potsdam M and Le Pape A. CFD investigations on a NACA0036 airfoil with active flow control. *Proc. 4th Flow Control Conference*, Seattle, Washington, USA, AIAA Paper 2008-3869, 2008.
- [9] Aubrun S Alvi F and Kourta A. Separation flow control on a generic ground vehicle using steady microjet arrays. *Proc. 5th Flow Control Conference*, Chicago, Illinois, USA, AIAA Paper 2010-4701, 2010.
- [10] Rivir R B, Sondergaard R, Bons J P and Yurchenko N. Control of separation in turbine boundary layers. *Proc. 2nd AIAA Flow Control Conference*, Portland, Oregon, USA, AIAA Paper 2004-2201, 2004.
- [11] Evans S, Hodson H, Hynes T, Wakelam C. and Hiller S-J. Controlling separation on a simulated compressor blade using vortex generator jets. *Proc. 4th Flow Control Conference*, Seattle, Washington, USA, AIAA Paper 2008-4317, 2008.
- [12] Ugrina S and Flatau A. Investigation of synthetic jet actuator design parameters. *Proc. Smart Structures and Materials 2004: Smart Structures and Integrated Systems*, San Diego, California, USA, Vol. 5390, pp 284-296, 2005.
- [13] Tesář V, Kordík J and Daněk M. *Lift and separation control on wind turbine blades by vortices having streamwise oriented axes*. Technical report, Institute of Thermomechanics ASCR v.v.i., Prague, October 2008.
- [14] Glezer A and Amitay M. Synthetic jets. *Annual Review of Fluid Mechanics*, Vol. 34, pp 503-529, 2002.
- [15] Widjanarko S M D, Geesing I J A K, de Vries H and Hoeijmakers H W M.: Experimental/Numerical Investigation Airfoil with Flow Control by Synthetic Jets. *Proc. 28th Congress of the International Council of the Aeronautical Sciences ICAS 2012*. Brisbane, Australia, ICAS Paper 2012 ICAS 2012-3.7.5, 2012.
- [16] Cattafesta III L N and Sheplak M. Actuators for active flow control. *Annual Review of Fluid Mechanics*, Vol. 43, pp 247-272, 2011.
- [17] Oyarzun M A and Cattafesta L. Design and optimization of piezoceramic zero-net mass-flux actuators. *Proc. 5th Flow Control Conference*, Chicago, Illinois, USA, AIAA Paper 2010-4414, 2010.
- [18] Gomes L D, Crowther W D and Wood N J. Towards a practical piezoceramic diaphragm based synthetic jet actuator for high subsonic applications effect of chamber and orifice depth on actuator peak velocity. *Proc. 3rd AIAA Flow Control Conference*, San Francisco, California, USA, AIAA Paper 2006-2859, 2006.
- [19] Jabbal M Liddle S, Potts J and Crowther W. Development of design methodology for synthetic jet actuator array for flow separation control applications. *Proc. 6th AIAA Flow Control Conference*, New Orleans, Louisiana, USA, AIAA Paper 2012-3242, 2012.
- [20] Glezer A, Amitay M and Honohan A M. Aspects of low- and high-frequency actuation for aerodynamic flow control. *AIAA Journal*, Vol. 43, pp 1501-1511, 2005.
- [21] McCormick D C. Boundary layer separation control with directed synthetic jets. *Proc. 38th AIAA Aerospace Sciences Meeting and Exhibit*, Reno, Nevada, USA, AIAA Paper 2000-0519, 2000.
- [22] Tian Y, Song Q and Cattafesta L. Control techniques for flows with large separated regions: A new look at scaling parameters. *Proc. 3rd AIAA Flow Control Conference*, San Francisco, California, USA, AIAA Paper 2006-2857, 2006.
- [23] Gressick W, Maldonado V, Farnsworth J and Amitay M. Active enhancement of wind turbine blades performance. *Proc. 46th AIAA Aerospace Sciences Meeting and Exhibit*, Reno, Nevada, USA, AIAA Paper 2008-1311, 2008.
- [24] Ingard U. On the theory and design of acoustic resonators. *The journal of the acoustical society of America*, Vol. 25, pp 1037-1061, 1953.
- [25] Mane P, Mossi K, Rostami A, Bryant R and Castro N. Piezoelectric actuators as synthetic jets: Cavity dimension effects. *Journal of Intelligent Material Systems and Structures*, Vol. 18 pp 117-119, 2007.
- [26] Duvigneau R, Hay A and Visonneau M. Study on the optimal location of a synthetic jet for stall control. *Proc. 3rd AIAA Flow Control Conference*, San Francisco, California, USA, AIAA Paper 2006-3679, 2006.
- [27] van Rooij R P J O M. *Modification of the boundary layer calculation in RFOIL for improved airfoil stall prediction*. Technical report, NLR, September 1996.

- [28] Drela M. XFOIL 6.9 *User Guide*. MIT Aero & Astro Harold Youngren, Aerocraft, Inc., January 2001.
- [29] Bosschers J. *Modelling of rotational effects with a 2-D viscous-inviscid interaction code*. NLR, Technical Report CR 96521, 1996.
- [30] Kim M, Lee B, Kim C and Jung K J. Numerical study on flow characteristics of synthetic jets with rectangular and circular exits. *Proc. 6th AIAA Flow Control Conference*, New Orleans, Louisiana, USA, AIAA Paper 2012-3049, 2012.
- [31] Yang A-S. Design analysis of a piezoelectrically driven synthetic jet actuator. *Smart Materials and Structures*, Vol. 18, No. 12, 2009.
- [32] Kim Y H and Garry K P. Optimization of a rectangular orifice synthetic jet generator. *Proc. 3rd AIAA Flow Control Conference*, San Francisco, California, USA, AIAA Paper 2006-2862, 2006.
- [33] Mossi K and Bryant R. Characterization of piezoelectric actuators for flow control over a wing. *Proc. 9th International Conference on New Actuators*, Bremen, Germany, June 2004, pp 181-185
- [34] Amitay M and Glezer A. Role of actuation frequency in controlled flow reattachment over a stalled airfoil. *AIAA Journal*, Vol. 40, No. 2, pp 209-216, 2002.
- [35] Vasile J and Amitay M. Interaction of a finite-span synthetic-jet and a cross-flow over a swept-back finite wing. *Proc. 6th AIAA Flow Control Conference*, New Orleans, Louisiana, USA, AIAA Paper 2012-2948, 2012.
- [36] Koopmans E. *Experimental study on flow separation control using synthetic jet actuators*. MSc thesis University of Twente, June 2013.
- [37] Schüller M, Schulze R, Gebauer C, Lipowski M, Kaulfersch E, Nestler J, Otto T and Gessner T. Netzwerkmodellierung von doppelwandler Synthetic Jet Aktoren. *60. Deutscher Luft- und Raumfahrtkongress 2011*, Bremen, Germany, September 2011, pp 1185-1195.
- [38] Timmer W A. Two-dimensional low-Reynolds number wind tunnel results for airfoil NACA 0018. *Wind Engineering*, Vol. 32 pp 525-537, 2008.

give permission, or have obtained permission from the copyright holder of this paper, for the publication and distribution of this paper as part of the ICAS 2014 proceedings or as individual off-prints from the proceedings.

Contact Author Email Address

<mailto:h.w.m.hoeijmakers@utwente.nl>

Copyright Statement

The authors confirm that they, and/or their company or organization, hold copyright on all of the original material included in this paper. The authors also confirm that they have obtained permission, from the copyright holder of any third party material included in this paper, to publish it as part of their paper. The authors confirm that they